

Optical design of the Origins Space Telescope

James A. Corsetti,^{a,*} Joseph M. Howard,^a J. Scott Knight,^b and
Len Seals^{1b}^a

^aNASA Goddard Space Flight Center, Greenbelt, Maryland, United States

^bBall Aerospace and Technologies Corp., Boulder, Colorado, United States

Abstract. Our paper discusses the optical design of the *Origins* Space Telescope. *Origins* is one of four large missions under study in preparation for the 2020 Decadal Survey in Astronomy and Astrophysics. Sensitive to the mid- and far-infrared spectrum (between 2.8 and 588 μm), *Origins* sets out to answer a number of important scientific questions by addressing NASA's three key science goals in astrophysics. The *Origins* telescope operates at $f/14$. The design includes a 5.9-m-diameter primary mirror. The large on-axis primary consists of 18 "keystone" segments of two different prescriptions arranged in two annuli (six inner and twelve outer segments) that together form a circular aperture in the goal of achieving a symmetric point spread function. To accommodate the 46×15 arc min full field of view (FOV) of the telescope at the design wavelength of $\lambda = 30 \mu\text{m}$, a three-mirror anastigmat configuration is used. The design is diffraction-limited across its instruments' FOV. A brief discussion of each of the three baselined instruments within the Instrument Accommodation Module is presented: (1) *Origins* Survey Spectrometer, (2) Mid-infrared Spectrometer, Camera transit spectrometer channel, and (3) Far-Infrared Polarimeter/Imager. In addition, the upscope options for the observatory are laid out as well including a fourth instrument: the Heterodyne Receiver for *Origins*. © The Authors. Published by SPIE under a Creative Commons Attribution 4.0 Unported License. Distribution or reproduction of this work in whole or in part requires full attribution of the original publication, including its DOI. [DOI: [10.1117/1.JATIS.7.1.011010](https://doi.org/10.1117/1.JATIS.7.1.011010)]

Keywords: optics; *Origins*; infrared; segmented mirror; cryogenic; decadal; imaging; spectroscopy.

Paper 20078SS received Jun. 15, 2020; accepted for publication Dec. 16, 2020; published online Feb. 3, 2021.

1 Introduction

Portions of this paper appear in the *Origins* Study Final Report.¹

The *Origins* Space Telescope (*Origins*) traces our cosmic history, from the formation of the first galaxies and the rise of metals to the development of habitable worlds and present-day life. *Origins* does this through exquisite sensitivity to infrared radiation from ions, atoms, molecules, dust, water vapor, and ice, and observations of extra-solar planetary atmospheres, protoplanetary disks, and large-area extragalactic fields. *Origins* operates in the wavelength range 2.8 to 588 μm and is more than 1000 times more sensitive than its predecessor Herschel due to its large, cold (4.5 K) telescope, and advanced instruments.

Origins is one of four large missions currently under study for the 2020 Decadal Survey in Astronomy and Astrophysics.^{1,2} Sensitive in the mid- and far-infrared spectrum (between 2.8 and 588 μm) and estimated to launch in approximately 2035 if selected in the Decadal Survey. *Origins* is designed to address NASA's three key astrophysics science goals: "How does the universe work?," "How did we get here?," and "Are we alone?" To do so, *Origins* seeks to answer three main questions:

1. How do galaxies form stars, build up metals, and grow their central supermassive black holes from reionization to today?
2. How do the conditions for habitability develop during the process of planet formation?
3. Do planets orbiting M-dwarf stars support life?

*Address all correspondence to James A. Corsetti, james.a.corsetti@nasa.gov

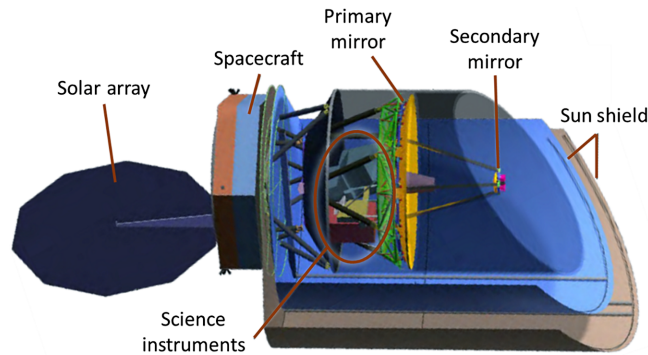


Fig. 1 Structural model of the *Origins* space telescope observatory.

As shown in Fig. 1, *Origins* has a Spitzer-like architecture with fixed baffles and simplified deployment for the sun shields. The observatory is designed with a modular instrument bay that facilitates integration and test and allows potential serviceability of the current instruments or potential replacement with new ones. Figure 1 shows the telescope itself with the science instruments sitting directly behind the primary mirror. The locations of the spacecraft, solar array, and deployed sun shield are indicated as well. *Origins* will be deployed at the Sun–Earth L2 Lagrange point.

2 Telescope Optical Design

2.1 Design Form

As shown in Fig. 2, the *Origins* telescope is a three-mirror anastigmat (TMA) with a field-steering mirror (FSM). This four mirror design includes three powered mirrors of different conic shapes (the elliptical primary, hyperbolic secondary, and elliptical tertiary mirrors) and a flat FSM. The TMA is the same general optical design form that has been proven on James Webb Space Telescope (JWST) and is well understood. An initial, off-axis optical design considered for a previous iteration of *Origins* [with a larger aperture and field of view (FOV)] resulted in a TMA with a “freeform” surface on all four mirrors to assist in correction of optical aberrations. After both aperture and FOV were reduced for size and packaging reasons, later

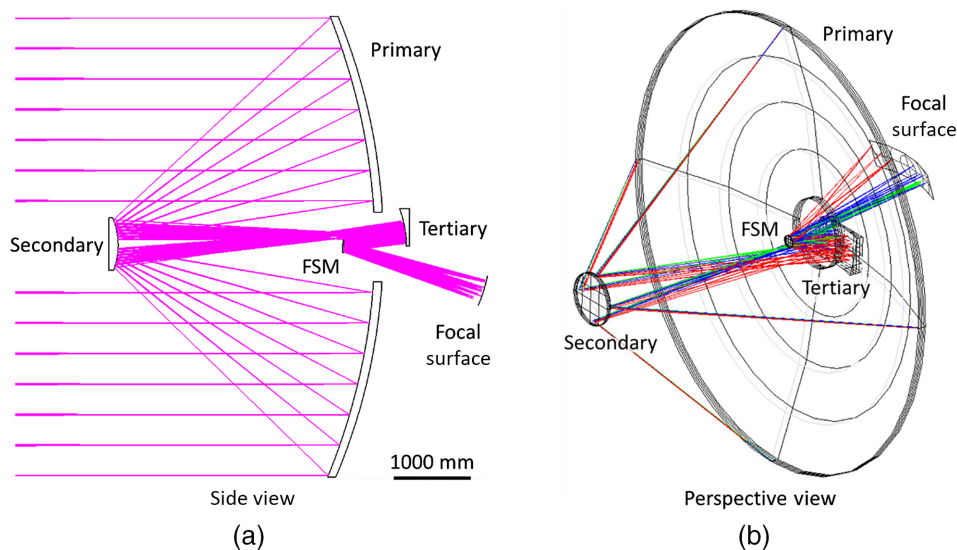


Fig. 2 *Origins* baseline telescope layout shows the locations of the four mirrors and focal surface from both (a) side and (b) perspective views.

studies found both the freeform and off-axis design aspects to be costly and more challenging to implement, and so the design was modified. Other benefits of choosing the on-axis architecture over the off-axis one include avoiding a secondary mirror that requires deployment on orbit, as well as allowing the instrument volume to fit compactly behind the primary mirror. As such, the final baseline design was constrained to have an on-axis pupil (obstructed primary mirror). The obstructed primary mirror also made the observatory simpler to package in the fairing as compared to studies regarding a telescope with an unobstructed primary mirror. The unobscured telescope was more desirable from a scientific standpoint (maximizing throughput); however, the packaging/deployment considerations made the obscured system more desirable. While a number of aperture shapes were investigated for the purpose of this design study (based on the goal of trying to find the one easiest to package and deploy), ultimately a circular aperture was chosen as it yielded the point spread function with the least effects of diffraction while being possible to fit it already fully deployed within the chosen fairing before launch. This fact is a major benefit of the telescope design as the lack of deployments leads to lower risk and reduced cost. Once in space, actuators for each primary mirror segment enable final alignment during commissioning with each segment able to adjust in three degrees of freedom (tip, tilt, and piston). Requirements for the *Origins* telescope are summarized in Table 1.

The primary mirror has 18 segments and is $f/0.63$ as shown in Table 1. A fast primary mirror is desirable for shortening the distance between the vertices of the primary and secondary mirrors (being approximately 3.33 m in the current design), therefore reducing the overall size of the observatory. Between the secondary and tertiary mirrors, the rays form an internal image (Cassegrain focus) that allows the tertiary mirror to image a real exit pupil. This real image will be surrounded by baffling to reject stray light. The FSM is placed at the exit pupil of the telescope, which actively tilts to control the FOV, directing it into each instrument as the observatory slowly drifts over the course of an observation. The FSM is used to provide fine control of the optical line of sight and to provide some rejection of internal disturbances. The telescope image surface is concave, with its center of curvature located at the FSM surface. Placing the FSM at the exit pupil (which is also at the center of curvature of the telescope image surface) prevents defocus from occurring during tilting of the FSM. This effectively makes a locally telecentric system for each field point, for which each chief ray is normal to the curved image surface.

Each mirror is assumed to be made of beryllium O-30-H with a density of 1.85 g/cm³. This material was chosen due to its high stiffness, low density, low coefficient of thermal expansion,

Table 1 Design requirements for the *Origins* space telescope.

Parameter	<i>Origins</i> baseline	Units
Primary diameter	Circular, 5.9	Meters
Primary hole diameter	0.9	Meters
Obscuration ratio	0.15	—
f -number	$f/14.0$ (telescope) $f/0.63$ (primary)	—
Effective focal length	82.6	Meters
FOV	46×15	Arc minute
Waveband	2.8–588	Microns
Operating temperature	4.5	Kelvin
Optical performance	Diffraction limited at $\lambda = 30 \mu\text{m}$	
Design form	TMA Obstructed (on-axis pupil)	
Mirror coatings	Protected gold	
Optical and structural material	Beryllium O-30-H	

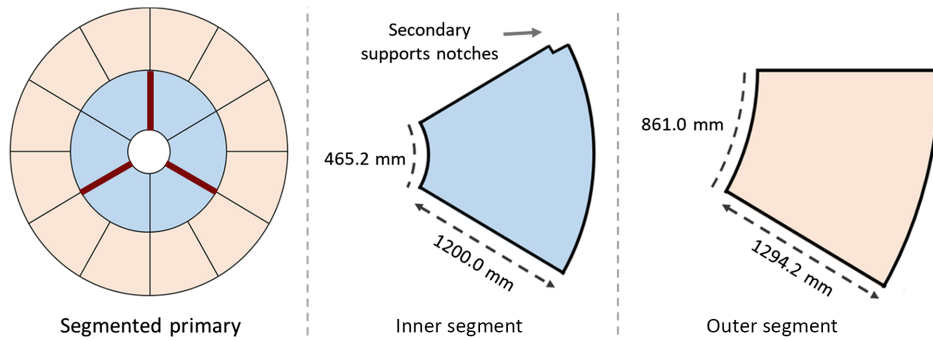


Fig. 3 Twelve *Origins* primary mirror outer segments are identical. The inner segments are of the same optical prescription, but with two variants on the location of the secondary support notch. The red bold lines in the leftmost picture indicate the secondary struts.

and high thermal conductivity and is baselined for the optical components and instrument structures throughout the observatory. Figure 3 shows dimensions for the six inner and twelve outer “keystone” segments that make up the primary mirror. Because the primary mirror is on-axis, all of the outer segments are identical. The inner segments have identical optical prescriptions; however, two variants are needed to accommodate a notch for the secondary mirror struts. Three of the inner mirror segments match the outline shown in Fig. 3, and three segments are reflections of this shape, with the notch in the opposite corner. The three secondary struts are designed to be in line with edge gaps between segments to minimize throughput loss. All four mirrors are gold-coated for improved reflectance in the infrared. Each mirror coating is assumed to have 98% reflectance and 2% emissivity, which is consistent with measurements made on JWST’s protected gold-coated mirrors up to a wavelength of $29 \mu\text{m}$.³ Non-JWST measurements on protected gold coatings in the terahertz regime have reported reflectance values around 99% between 100 and $600 \mu\text{m}$.⁴ Based on this, the total throughput for the *Origins* telescope is at least 92% with higher throughput at longer wavelengths.

2.2 Imaging Performance

The as-built *Origins* telescope is required to be diffraction-limited at a wavelength of $30 \mu\text{m}$. Root-mean-square (RMS) wavefront error is taken to be the metric by which performance is evaluated. A common standard for diffraction-limited performance is to have less than 0.07λ of wavefront error. For a design wavelength of $30 \mu\text{m}$, this corresponds to less than $2.1 \mu\text{m}$ RMSWE. Figure 4 shows that this specification is met across the telescope’s and therefore each instrument’s FOV. The outlines of each instrument’s FOV (including all upscope options) are shown for reference. It is worth noting that the FOV is not symmetric around 0 deg in the x field direction. The reason for this is explained in further detail in Sec. 3. Table 2 summarizes the

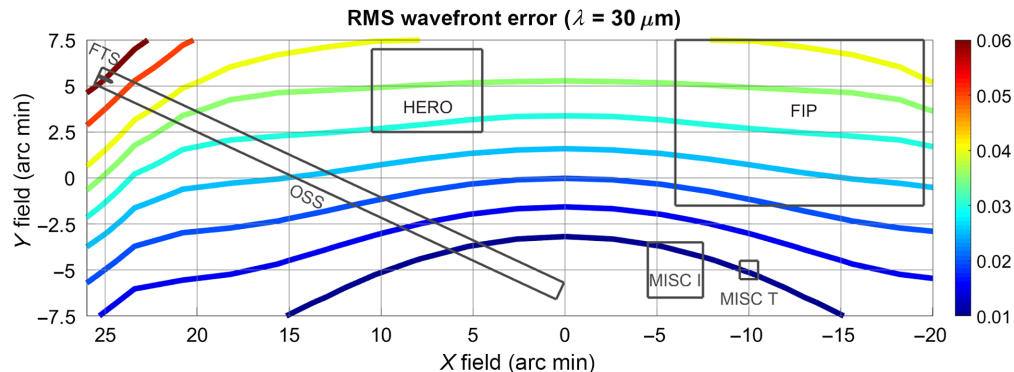


Fig. 4 Contour plot showing RMS wavefront error as a function of FOV for the *Origins* Space Telescope.

Table 2 Sensitivities of each of the three powered mirrors to six degree of freedom motion.

Tolerance	X	Y	Z	rX	rY	rZ
Units	(nm/ μ m)	(nm/ μ m)	(nm/ μ m)	(nm/arc sec)	(nm/arc sec)	(nm/arc sec)
Primary	12.5	12.4	76.6	224.5	225.1	0.0
Secondary	12.4	12.4	78.0	25.1	24.8	0.0
Tertiary	0.2	0.4	1.7	1.5	1.1	0.0

sensitivities of each of the three powered mirrors to six degree of freedom motion in units of accumulated nanometers of wavefront error per micron (for translations) or arc second (for rotations).

2.3 Stray Light Analysis

Stray light analysis refers to the process of identifying and preventing light rays from any source other than the object being observed, from reaching the detector plane. For this purpose, mechanical structures known as baffles are incorporated into the telescope design to block these unwelcome rays' potential "skip paths." Tight packaging constraints require careful consideration of how to adequately baffle against stray light. Often the constraints involved make it difficult to achieve well-separated paths from image and pupil conjugates, which would permit placement of effective baffles. As a result, baffling may be limited to careful use of pupil masks and baffles combined with field masks at or near-intermediate images to restrict specular paths from the sky to the focal plane other than from within the FOV. The stray light analysis of *Origins* was carried out in FRED software.

Figure 5 shows *Origins*' external and internal baffling. The external baffling is shown in red in Fig. 5(a) while Fig. 5(b) shows the "snout" baffling and vanes that are coming away from the hole in the primary mirror toward the secondary mirror. Figure 6 shows the effectiveness of the baffling in blocking stray light. In each case, rays were traced backward through the system from the instrument FOV footprints at the focal surface toward the primary and onto the sky. In Fig. 6, the rays leaving the focal surface are colored green and remain so until reflecting off of the tertiary mirror, at which point they are colored red. In Fig. 6(a) (without baffling), there is a significant ray path that allows light to travel directly from the focal surface to the sky without hitting the tertiary (as evident from the fact that the rays remain green in color). In Fig. 6(b), the baffling blocks this skip path and only the desired FOV (the red rays) make it all the way from the image surface to the sky. Figure 7 shows the intensity signal-to-noise ratio between the desired FOV allocated to the instruments and noise due to scatter. Figure 7 shows that the difference between the two is between about 4 and 5 orders of magnitude. This value can be further reduced

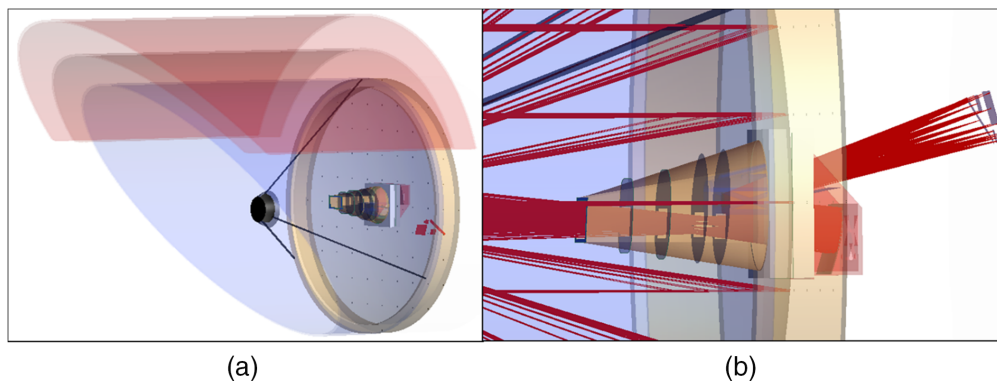


Fig. 5 (a) External and (b) internal baffles. Both sets of baffling are meant to prevent unwanted light from reaching the focal surface.

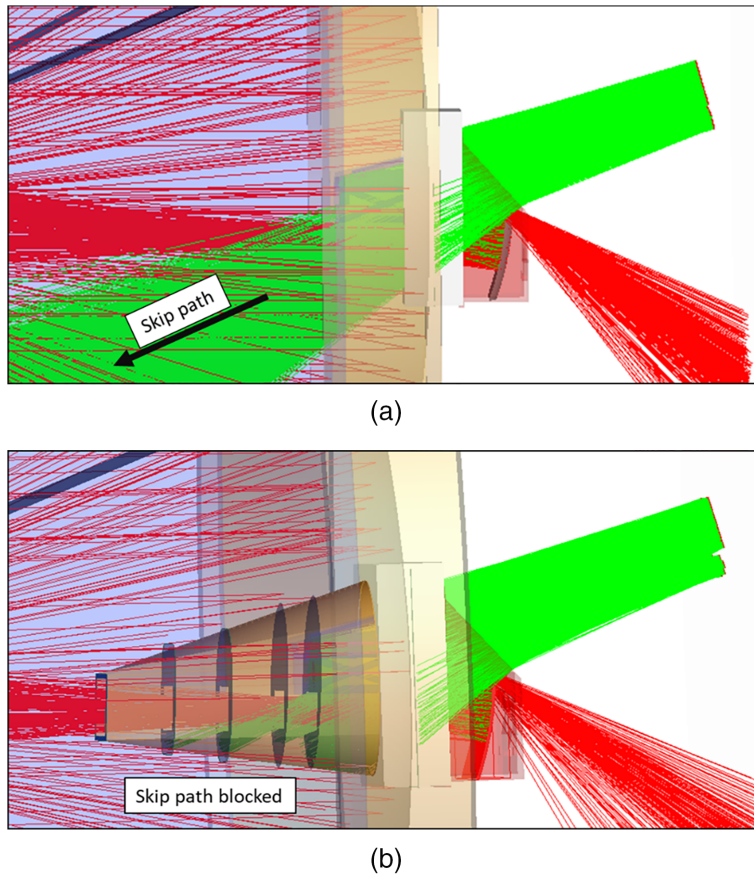


Fig. 6 Images showing the effect of baffling to mitigate stray light. (a) No baffling allows for skip ray paths and light to travel directly from the sky to focal surface without reflecting off the telescope mirrors versus (b) having baffling, which prevents this from occurring.

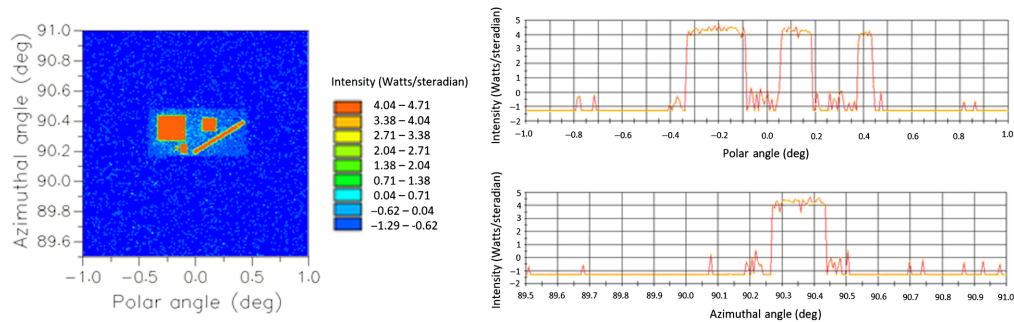


Fig. 7 Analysis showing relative intensity between the desired signal (the instruments' FOV footprints) and noise due to near-field scatter. It is worth noting that the x and y line scans are plotted on a logarithmic scale and show between about 4 and 5 orders of magnitude difference between signal and noise. Calculations carried out at $\lambda = 30 \mu\text{m}$.

by adding further baffles. As the FSM is located at the exit pupil of the telescope, an image of the primary mirror forms there. To further mitigate stray light, it is useful to place a baffle around the FSM, as was the case for the FSM of JWST.

In addition to blocking skip paths as mentioned above, scatter is another consideration in stray light analysis. Scatter can be reduced using mirrors that are well polished with low surface roughness as well as clean. In the FRED nonsequential ray trace model of the telescope, surface

roughness is represented by the Harvey–Shack model with particulate contamination modeled by MIL-STD-1246C. Figure 8 shows the effect of surface roughness in more detail. By increasing the surface roughness of the primary mirror from 1.5 to 15 to 100 nm (while leaving the secondary, tertiary, and FSM each with a surface roughness of 1.5 nm in each case), it is apparent that a rougher surface leads to a worsened signal-to-noise ratio between on- and off-axes. This is due to the increased scatter. The bottom plot of Fig. 8 shows the case for which the primary mirror has again a surface roughness of 1.5 nm but no longer includes any baffling. Further design studies will determine the final requirements on surface roughness. To limit thermal radiation from the telescope, a combination of high-emissivity coatings, Ball InfraRed Black™, and low temperature is employed throughout the design of the observatory. The cooling system utilizes a combination of passive cooling provided by a two-layer deployed sunshield, a single stage radiator at 35 K, and four mechanical cryocoolers in operating in parallel. The thermal design of *Origins* enables a transition between 280 K at the outer sunshield, 119 K at the inner sunshield, 35 K at the barrel, 20 K at the middle zone, and 4.5 K for the instruments and telescope. For more information on the thermal design, see the *Origins* Final Report.¹

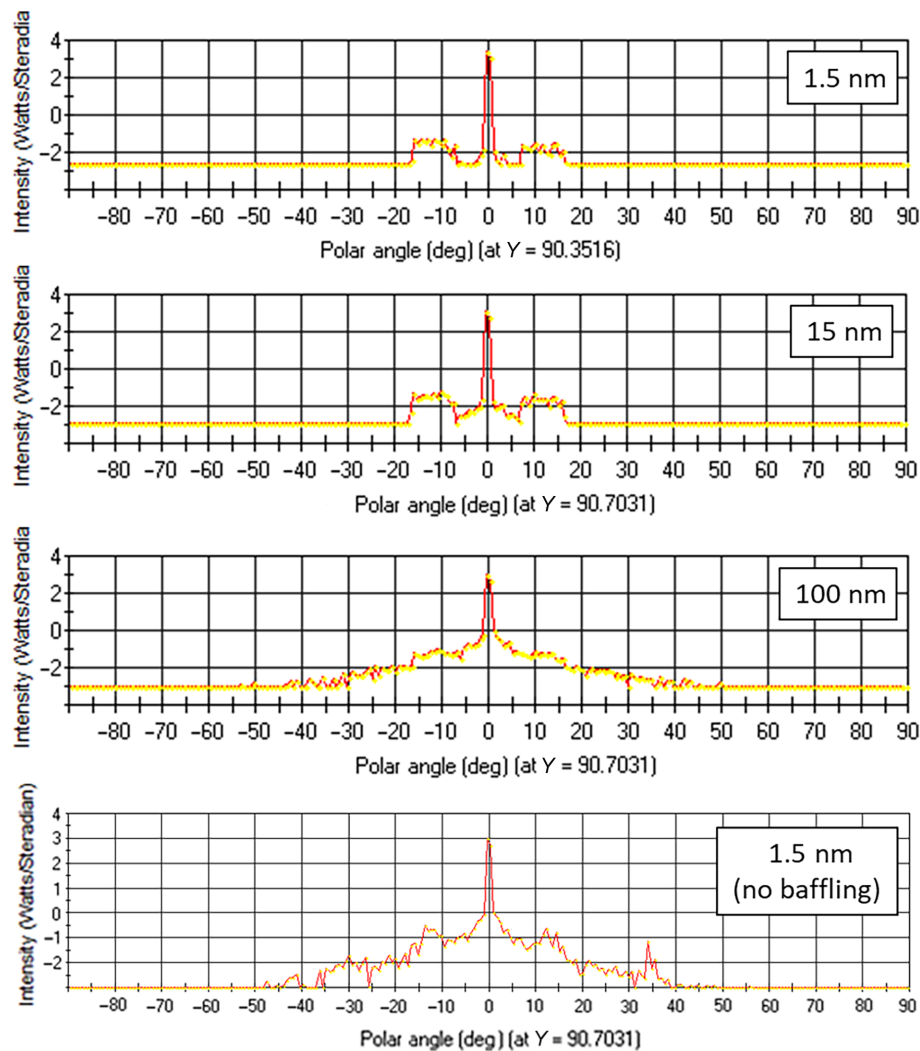


Fig. 8 The effect of primary mirror surface roughness on intensity as a function of FOV angle. As expected, as the primary mirror surface roughness increases, more scatter occurs from the surface, worsening the signal-to-noise ratio between on- and off-axes. The intensity scales are logarithmic. Calculations carried out at $\lambda = 30 \mu\text{m}$.

3 Instruments

The baseline *Origins* design contains three instruments. These are: (1) the *Origins* Survey Spectrometer (OSS),⁵ (2) the Mid-Infrared Spectrometer (Camera) Transit Spectrometer (MISC-T),^{6,7} and (3) the Far-Infrared Polarimeter/Imager (FIP).⁸ OSS is the primary science instrument with six grating modules to enable simultaneous spectroscopic measurements between 25 and 588 μm at a resolving power (R) of 300. In addition to the grating modules, OSS provides two high resolution modes: a Fourier-transform spectrometer and an etalon, which enable $R = 30,000$ and $R = 200,000$ measurements, respectively, over narrower spectral ranges. MISC is a densified pupil spectrometer that provides R values between 50 and 295 over a spectral range between 2.8 and 20 μm for transiting exoplanet spectroscopy with very high spectrophotometric stability. FIP serves the role of the observatory’s large FOV imager, providing both traditional imaging and polarimetry measurements.

Figure 9 shows the FOV allocations for each of the three baselined instruments. As mentioned previously, the telescope is designed over a rectangular 15×46 arc min full FOV; however, this FOV is not symmetric, being longer in the direction of OSS than FIP. This is due to the fact that during the design process, further FOV was added to OSS after the FIP design had been completed. Rather than redesign FIP at that stage, OSS’s FOV was extended in the direction away from the center of the FOV. This asymmetry can be addressed in a later design by just shifting both instruments’ designated FOVs by approximately 3 arc min. In Fig. 9, 1 arc min of FOV on the sky corresponds to about 24 mm in length at the focal surface. Space for mounting structures is left between the instruments. Looking at Fig. 9, there is a large amount of space between the different instruments in the x direction of the FOV. This is to make it possible to more easily accommodate any desired upscoopes to the *Origins* baseline design. Optional upscoopes include: greater FOV for both OSS and FIP, another channel for MISC, and the addition of the Heterodyne Receiver for *Origins* (HERO) instrument. In future design iterations, once the total number of instruments and FOV allocations for each instrument is decided, the footprints in Fig. 9 would be reoptimized to make better use of the central “sweet spot” of optical performance and reduce the large gaps between instruments. Figure 10 shows a CODEV[®] layout showing rays for each of the three baseline instruments passing through the telescope onto the image surface. FIP plays a critical functional role in aligning the mirrors during on-orbit commissioning. All of the instruments, including details on optical design, are discussed in greater detail in the *Origins* Final Report.¹

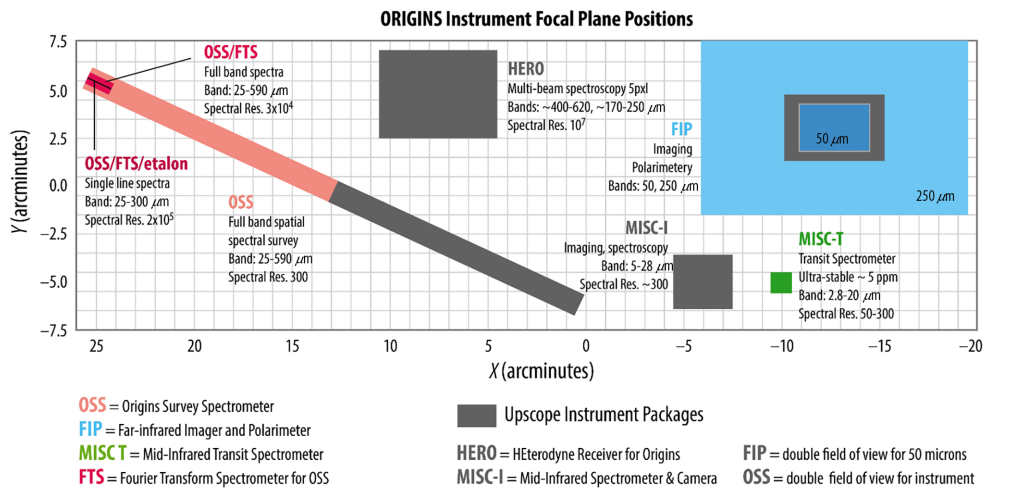


Fig. 9 FOV allocations for each of the *Origins* instruments.

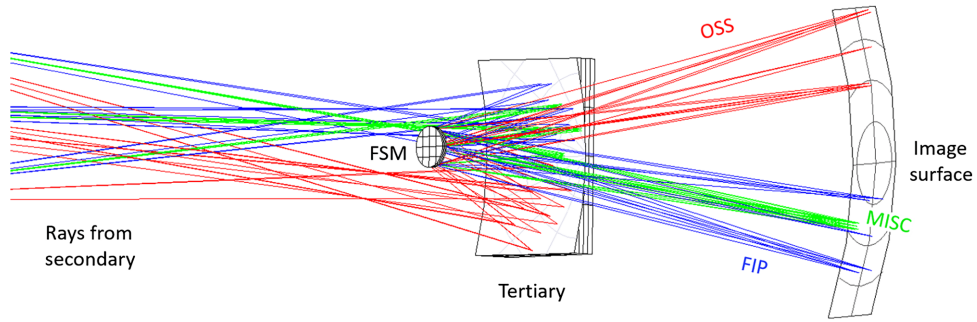


Fig. 10 Ray trace showing the light reflecting from the FSM to *Origins* image surface and individual instruments.

3.1 Optical Error Budget

An error budget for this telescope has been developed and is shown in detail. This document lays out the allocation of wavefront error to design, thermal stability, line of sight/jitter, and reserve for each of the instruments and the telescope itself.

This section presents the optical error budget carried out in conjunction between NASA Goddard and Ball-Aerospace in detail. The purpose of such a budget is to identify different sources that can all contribute to the wavefront error of the telescope and ensure that the diffraction-limited performance specification is still met. Given the design wavelength of $30\ \mu\text{m}$ and a Strehl ratio of 0.8, the goal as-built RMS wavefront error is 2255 nm. Figure 11 shows that the terms, when root summed squared together, do indeed meet the 2255 nm requirement

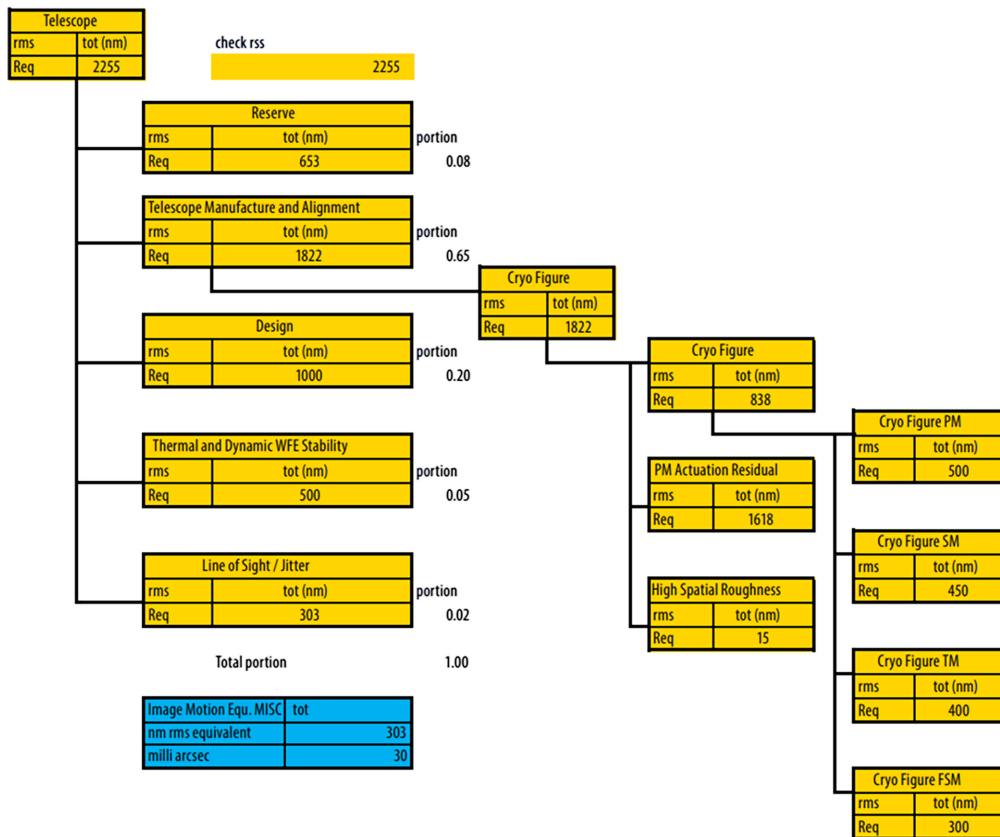


Fig. 11 Wavefront error budget for *Origins* telescope based on achieving diffraction-limited performance with the as-built telescope.

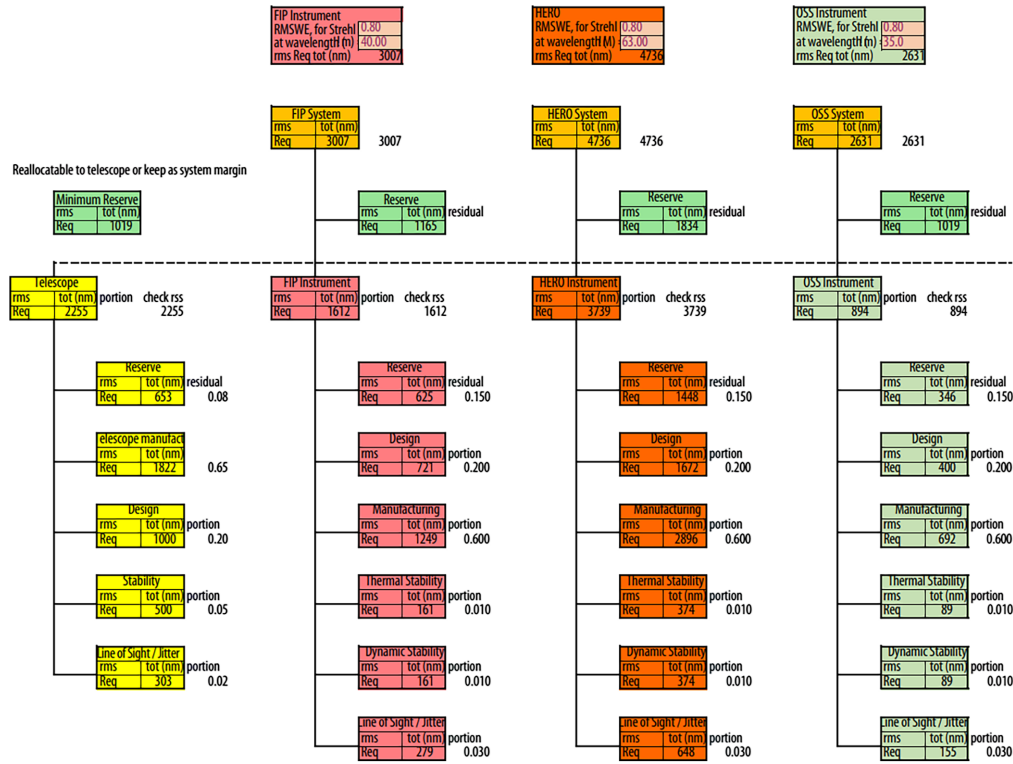


Fig. 12 Wavefront error budgets combining the allocations to the OSS, FIP, and HERO instruments with that of the telescope.

with the remainder designated as reserve. For future work, this wavefront budget would need to be broken into much greater detail, setting specific wavefront allocations for individual optical elements, field points, etc. Note that the design residual value of 1000 nm is greater than the amount of wavefront error shown across the majority of the FOV in Fig. 4. This number is meant to be a representative value across the entire FOV for the time being until more specific allocations as a function of FOV are developed in future budget revisions. Figure 12 shows a series of budgets combining the allocations to the OSS, FIP, and HERO instruments with that of the telescope. In each case, the top-level telescope wavefront budget value (2255 nm) is root summed squared together with the value from each instrument toward the desired value for the instrument/telescope combination based on its design wavelength. Any remainder is designated again as reserve. For example, FIP is to be diffraction-limited at a wavelength of 40 μm requiring a total RMS wavefront error 3007 nm. Root sum squaring the 2255 nm from the telescope with the 1612 nm calculated for the FIP instrument leaves over 1165 nm in reserve to total the top-level 3007 nm. For each instrument, the goal wavefront performance is met with reserve left over. It is worth noting that the MISC instrument is omitted from the budget since wavefront error is not the preferred metric for evaluation. Using simulated point spread functions generated in CODEV® (with a total of 2255 nm of wavefront error), the MISC team has concluded that the instrument achieves high stability due to small long-term drift and jitter.

4 Conclusions

In this paper, we presented an overview of the *Origins* Space Telescope observatory and the associated optical design.⁹ Details regarding optical performance including RMS wavefront error and stray light are presented, alongside an introduction to the *Origins* instruments. For more information on these topics, the reader is encouraged to read the *Origins* Final Report, which details the results of this study (see the documents link on Ref. 1).

References

1. “The Origins Space Telescope Study Team,” NASA Goddard, <https://asd.gsfc.nasa.gov/firs/> (2019).
2. D. Leisawitz, “The Origins Space Telescope,” *Proc. SPIE* **11115**, 111150Q (2019).
3. R. A. Keski-Kuha et al., “James Webb Space Telescope optical telescope element mirror coatings,” *Proc. SPIE* **8442**, 84422J (2012).
4. M. Naftaly and R. Dudley, “Terahertz reflectivities of metal-coated mirrors,” *Appl. Opt.* **50**, 3201–3204 (2011).
5. C. M. Bradford et al., “The Origins Survey Spectrometer (OSS): a far-IR discovery machine for the Origins Space Telescope,” *Proc. SPIE* **10698**, 1069818 (2018).
6. T. Matsuo et al., “A new concept for spectrophotometry of exoplanets with space-borne telescopes,” *Astrophys. J.* **823**, 139 (2016).
7. I. Sakon et al., “The mid-infrared imager, spectrometer, coronagraph (MISC) for the Origins Space Telescope (OST),” *Proc. SPIE* **10698**, 1069817 (2018).
8. J. Staguhn et al., “Origins Space Telescope: the far infrared imager and polarimeter FIP,” *Proc. SPIE* **10698**, 106981A (2018).
9. J. A. Corsetti et al., “Optical design of the Origins Space Telescope,” *Proc. SPIE* **11115**, 1111513 (2019).

James A. Corsetti is a member of the optical design group at NASA Goddard Space Flight Center in Greenbelt, Maryland. He received his BS, MS, and PhD degrees in optics from the Institute of Optics at the University of Rochester in 2010, 2013, and 2017, respectively.

Joseph M. Howard received his BS degree in physics from the US Naval Academy in Annapolis, Maryland, and his PhD in optical design from the Institute of Optics, University of Rochester, in Rochester, New York. He now serves as an optical designer for NASA, working on projects including the James Webb Space Telescope (JWST), the Roman Space Telescope, Origins, and the other future space missions.

J. Scott Knight is a mission systems engineer at Ball responsible for the optical architecture of large space missions. He has been involved with JWST for over 15 years concentrating on system analysis, system modeling, and ground-based verification. A portion of his responsibilities on JWST has included the management of optical performance analysis activities and leading the flight optical commissioning of the telescope. He also leads technology development at Ball Aerospace for space astrophysical missions.

Len Seals received his BS degree in physics from Grambling State University in Grambling, Louisiana, and his PhD in applied physics from the Georgia Institute of Technology. He now serves as a stray light analyst for NASA, working on projects including the JWST, the Roman Space Telescope, Origins, and the other future space missions.